[redacted]

FINAL - REC 5/6/96

CONF-9606115--6

SAND 96-0838C

PROPERTIES OF DYNAMICALLY COMPACTED WIPP SALT[1]

Nancy S. Brodsky, Frank D. Hansen
Sandia National Laboratories[2]
Albuquerque, NM USA

Tom W. Pfeifle
RE/SPEC, Inc.
Rapid City, SD USA

ABSTRACT

Dynamic compaction of mine-run salt is being investigated for the Waste Isolation Pilot Plant (WIPP), where compacted salt is being considered for repository sealing applications. One large-scale and two intermediate-scale dynamic-compaction demonstrations were conducted. Initial fractional densities of the compacted salt range from 0.85 to 0.90, and permeabilities range from approximately 10^{-12} m^2 to 10^{-15} m^2. Dynamically-compacted specimens were further consolidated in the laboratory by application of hydrostatic pressure. Permeability as a function of density was determined, and consolidation microprocesses were studied. Experimental results, in conjunction with modeling results (Callahan et al., 1996), indicate that the compacted salt will function as a viable seal material.

INTRODUCTION

The US Department of Energy (DOE) is planning to dispose of transuranic (TRU) wastes in bedded salt deposits at the Waste Isolation Pilot Plant (WIPP) near Carlsbad, New Mexico. The current mission of the WIPP is to provide a research and development facility to demonstrate the safe management, storage, and disposal of radioactive TRU waste resulting from US Government defense programs. The WIPP facility must demonstrate compliance with federal regulations in preparation for a Compliance Certification Application. Regulatory requirements include use of both engineered and natural barriers to limit migration of hazardous constituents to the regulatory boundary. The impetus for study of crushed salt reconsolidation derives from a need to design a permanent seal for WIPP repository shafts that provide access from the surface to the disposal area.

Seal system design activities at the WIPP have included extensive evaluation of several potential seal materials (US DOE, 1995). Most of the proposed seal materials are common construction materials such as concrete and asphalt. In addition, crushed salt is currently being proposed as a seal component to help permanently isolate the

facility. Although crushed salt has never been used as a seal material, it possesses several recognized attributes: (1) it is readily available because it is produced in large volumes during facility mining activities; (2) it is geochemically compatible with the host rock (i.e., halite); and (3) it will consolidate into a cohesive mass with low permeability as the sealed WIPP shafts creep inward. Fundamental issues for performance assessment include understanding reconsolidation mechanisms, changes in permeability and density of the reconsolidated salt over time, and emplacement density required to meet regulatory performance standards.

To design and evaluate performance of a compacted salt column, three avenues of basic and applied research were pursued:

- Establish initial conditions by demonstrating potential construction techniques and determining density and permeability of salt as it is expected to compact in a shaft.
- Perform requisite laboratory tests to evaluate the relationship between permeability and density, measure mechanical properties, and document deformational processes.
- Develop a constitutive model for consolidating crushed salt to be used both in design and performance assessment.

The DOE directed Sandia National Laboratories to embark on a program to address fundamental questions concerning crushed salt placement in a shaft, its subsequent consolidation, and numerical modeling of its long-term performance assessment. In general, the activities are divided into field demonstrations, laboratory testing, and constitutive model development. The three areas are summarized in three papers in these *Proceedings*. This paper summarizes the laboratory testing, and the compaction demonstration and the constitutive model are summarized in Hansen and Ahrens and Callahan et al., respectively. Advancements in these three areas have provided assurance that compacted salt will function as a viable seal for the WIPP.

EXPERIMENTAL PROGRAM

Dynamic Compaction Tests

Dynamic compaction was conducted in a surface-based operation in which heavy tampers were successively dropped into a steel chamber containing mine-run WIPP salt. The compacted salt served as starting material for laboratory testing. The experimental program first established density and permeability of the dynamically compacted crushed salt mass (initial conditions possible for the shaft seal element) and then consolidated the tamped salt further while measuring density, permeability, and elastic moduli. Microscopy was used to describe the tamped material and to determine consolidation mechanisms.

Subject samples were derived from three dynamic-compaction demonstrations conducted at Sandia National Laboratories in Albuquerque, NM. A basic summary of compaction information is given in Table I. A steel chamber 1.8 m high and 1.2 m in diameter (intermediate scale) or 3.7 m high and 3.7 m in diameter (large scale) was

filled with a known mass and volume of mine-run crushed WIPP salt. The salt was placed into the chamber in successive lifts, which were then compacted by the repeated dropping of a cylindrical tamper into the steel chamber. The number of tamper drops was determined so that the compaction effort for each lift approximated two or three times Modified Proctor Energy (MPE). During the first demonstration, the third MPE was observed to cause very little additional compaction, so only two MPE were applied for the second intermediate-scale demonstration. Deeper lifts were subjected to additional compaction energy as upper lifts were tamped. Impact of the tamper pulverized the salt surface. This powder remained on top of a lift when the next lift was placed and compacted to a very high density during subsequent tamping.

Table I. Dynamic Compaction Demonstration Summary

	First Dynamic Compaction Demonstration (Intermediate Scale)	Second Dynamic Compaction Demonstration (Intermediate Scale)	Third Dynamic Compaction Demonstration (Large Scale)
Moisture Content			
Targeted	As is	1 % Added	1 % Added
Measured	0.26 %	1.27 %	0.33 – 0.67 % [a]
Lifts			
Number	2	2	3
Height per lift (m)	0.9	0.9	1.5
Modified Proctor Energy per lift	3	2	3

[a] 1.0 % upon emplacement in chamber; these drier samples resulted from about 100 days at 25° C.

For the first demonstration, the moisture content of the mine-run salt was "as is" (0.26 %), whereas an additional 1.0 % moisture was added to the uncompacted salt for the second and third demonstrations. After the field demonstrations were completed, the compacted salt mass was sawed into blocks, and several blocks were shipped to RE/SPEC Inc. for testing.

Specimen Preparation

Test specimens were prepared by machining blocks of dynamically compacted salt into right circular cylinders nominally 102 mm (4 inches) in diameter and 102 mm to 203 mm (4 to 8 inches) in length. All coring was performed under dry conditions.

Sample material from the first dynamic compaction demonstration (DC1) consisted of nine blocks from which five cylindrical test specimens were prepared. Attempts to prepare specimens from all but the most dense sample blocks failed due to lack of cohesion. The original orientation was not marked on the blocks, but a vertical axis was hypothesized based on the grain fabric.

A shipment from the second dynamic compaction demonstration (DC2) contained 11 sample blocks and additional sample material in three 102-mm-diameter PVC tubes. These samples appeared to be more cohesive than those in the first shipment, and four test specimens were prepared from this material. Coring locations were chosen so that extremes in density would be sampled. Two specimens were taken from a location as close as possible to the outer margin of the chamber, and two specimens were taken from near the center. Again, the specimen axes were vertical.

Sample material from the large-scale dynamic compaction demonstration (DC3) comprised three large blocks (approximately 0.5-m cubes) and additional material cored *in situ* (i.e., cored before the compacted salt was sawed into blocks) in preparation for gas permeability tests on the compacted mass itself. Four horizontal (taken perpendicular to the direction of dynamic compaction) and five vertical specimens were obtained from the large blocks. Vertical heterogeneity gave rise to disk-shaped cores with lengths from 25 to 150 mm, while the horizontal coring generally yielded a single intact core about 200 to 250 mm in length. An additional single test specimen was prepared from material cored *in situ*. Moisture contents were measured for samples from both the large blocks and the material cored *in situ*.

Laboratory Test Methods

Density and moisture content. Laboratory test methods for density and moisture content were straightforward. Density determinations required the measurement of specimen mass and volume. All masses were determined using a Sartorius balance with an accuracy of 0.01 g. Specimen dimensions were measured using calipers and a height gage. Moisture contents were determined by drying samples at 110° C until masses were stable (to within 0.01 g) for over 24 hours.

Permeability. Permeability tests were conducted in a pressure vessel and load frame assembly. This test system included components for control and monitoring of axial force, confining pressure, and temperature. Axial and volumetric strains were monitored with linear variable differential transformers and a dilatometer system, respectively (Brodsky, 1994). The transducers used to collect force, pressure, deformation, and temperature data were calibrated using documented procedures and standards traceable to the National Institute of Standards and Technology.

Two measurement systems were used for gas permeability measurements; both are described in Hansen et al. (1995). The first method was designed for low permeability specimens and used a manometer system for measuring gas flow. The second method, commonly used for higher permeability materials, used a flow tube meter for measuring gas flow. For tests conducted using the manometer-type permeability system, three values of inlet pressure were used when possible so that the relationship between flow rate and pressure difference across the specimen could be monitored for linearity. (A linear relationship implies that flow is laminar.) The data were corrected for slippage effects using the Klinkenberg (1941) correction by plotting permeability versus reciprocal mean pore pressure and fitting a straight line to the data. The perme-

ability axis intercept at a reciprocal mean pressure of zero gives the equivalent liquid permeability value.

The specimen assembly is shown in Figure 1. Permeant entered the system through the lower platen, permeated the specimen, and exited through the upper vent. Spacers were used to extend the lengths of shorter specimens so that they could be accommodated by the testing machine. Porous felt-metal disks were placed along the specimen/platen interfaces to ensure uniform permeant pressure along the specimen's upper and lower surfaces. Viton jackets or sleeves were used to protect specimens from the silicone oil used as a confining fluid.

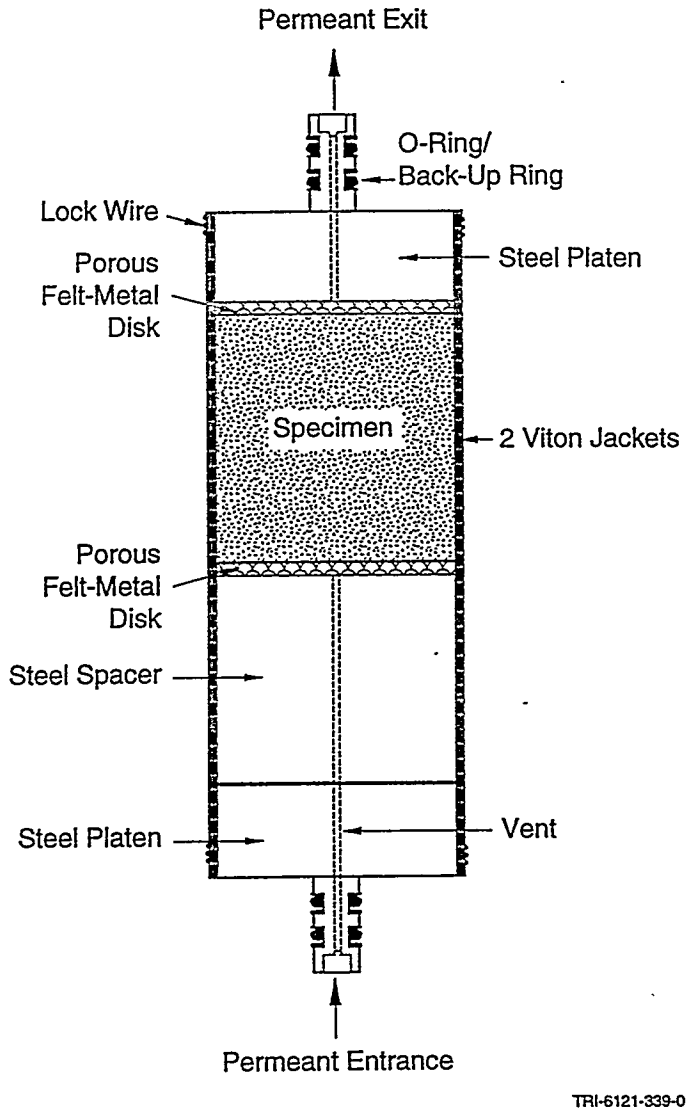

Figure 1. Specimen Assembly for Permeability Tests.

Elastic Moduli. One specimen from DC3 was subjected to a complex load path so that elastic moduli and permeability could be measured as a function of increasing density (see Figure 2). The specimen was subjected to repeated cycles of hydrostatic consolidation at elevated pressures (10 and 15 MPa) followed by permeability and standard triaxial compression tests at low pressure (1 MPa). Triaxial compression tests were conducted at constant strain rate to a maximum axial stress difference of 5 MPa.

RESULTS

Density

Density data are presented as fractional values, i.e., measured density normalized to the density of intact salt (2,160 kg/m^3). Sample fractional densities from the first, second, and third dynamic compaction tests ranged from 0.86 to 0.91, 0.85 to 0.90, and 0.89 to 0.91, respectively, which is considered very encouraging for compacted salt seal applications. Overall these data show that fractional densities in excess of 0.85 and generally above 0.90 can be achieved by dynamic compaction. This result is most encouraging because no optimization was undertaken. With simple changes to the compaction process, such as crushing mine-run salt to a smaller maximum grain size and perhaps adding slightly more water, it is possible that densities on emplacement in a shaft seal could exceed 0.90.

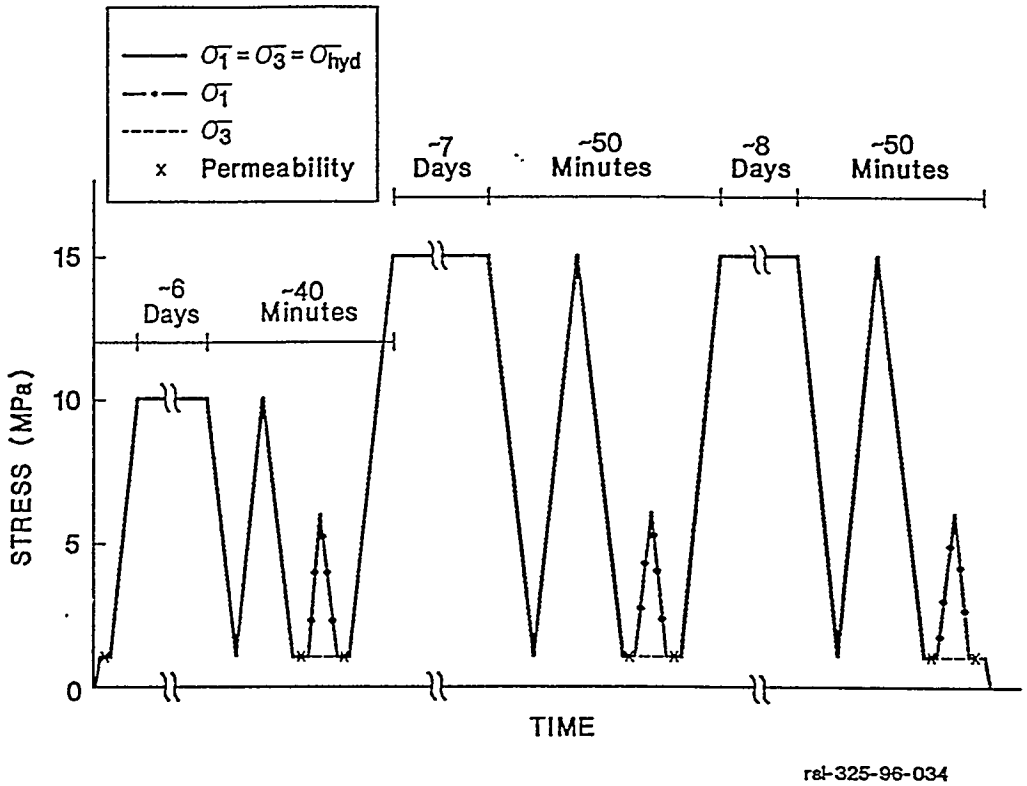

Figure 2. Loading Path for Reconsolidated Crushed Salt Specimen.

Permeability

Permeability and density data are shown in Figure 3. In addition to laboratory data from the dynamic compaction demonstrations, this plot includes (1) an average measurement of gas permeability (9×10^{-14} m^2) made *in situ* during the third or large-scale dynamic compaction demonstration and (2) measurements of brine permeability in crushed salt (Brodsky, 1994). The data in Figure 3 show a reasonably consistent relationship between permeability and fractional density for crushed salt. All data were fit (log of permeability versus fractional density) using a linear least-squares regression to obtain an average decrease of 5.49 (± 0.56) orders of magnitude in permeability for a 0.1 increase in fractional density. The correlation coefficient for the fit (r^2) is 0.77.

Elastic Moduli

Fractional density versus time is shown in Figure 4 for the specimen from the DC3 demonstration. Note that the time axis for Figure 2 is discontinuous, whereas the time axis for Figure 4 is not. The specimen consolidated for approximately six days at 10 MPa hydrostatic pressure. Short unload/reload cycles (one hydrostatic cycle and axial loading cycle) were applied to determine bulk modulus and Young's modulus, respectively. Hydrostatic pressure was then increased to 15 MPa, and a corresponding increase in densification was observed. Two additional unload/reload cycles were performed as shown to obtain elastic moduli at higher densities.

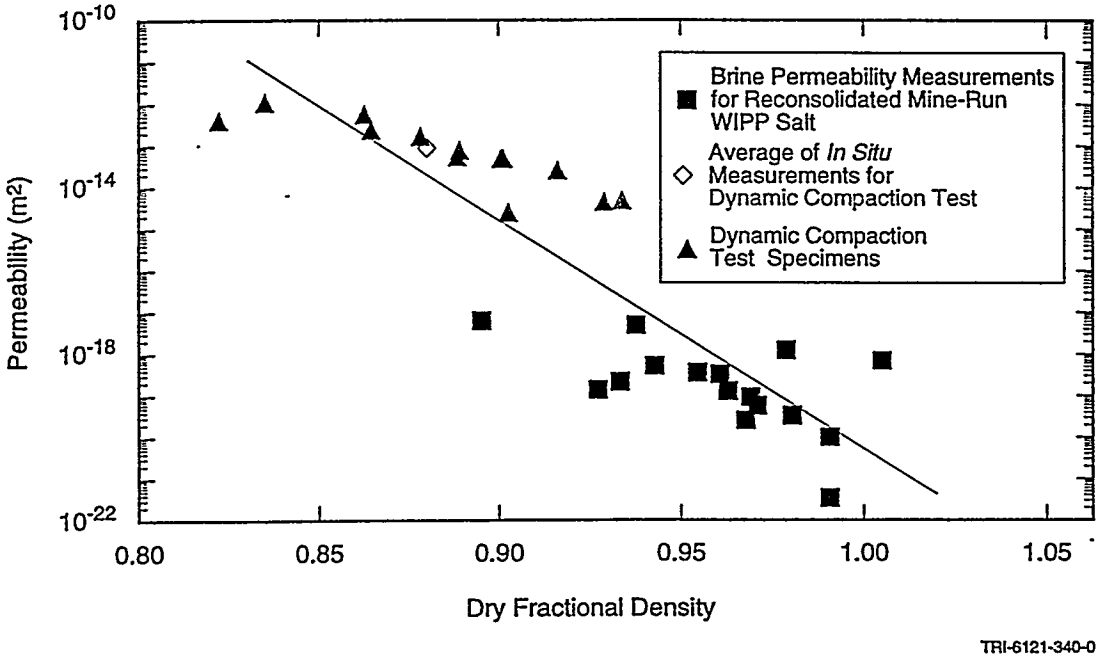

Figure 3. Permeability of Crushed Salt versus Fractional Density.

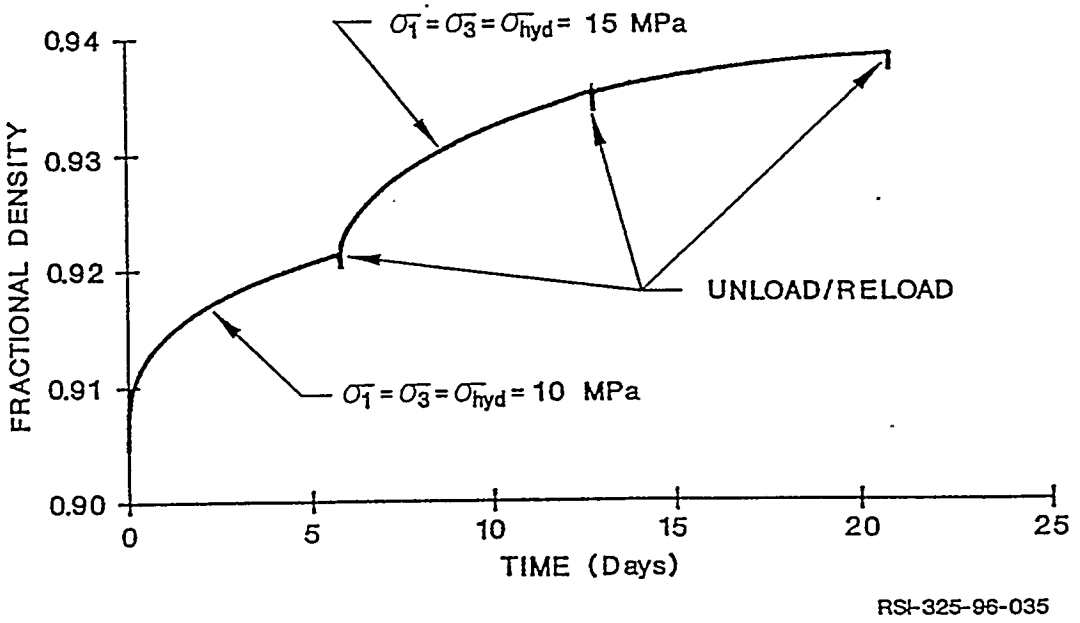

Figure 4. Changes in Fractional Density for Reconsolidated Crushed Salt Specimen.

Young's moduli increased with increasing fractional density and values of 18.9, 21.7, and 22.5 GPa were obtained for the three axial loading cycles, respectively.

Bulk moduli obtained for this specimen are shown in Figure 5 as a function of specimen density. The modulus for intact WIPP salt and moduli for non-WIPP Permian basin salt at lower densities obtained by Holcomb and Hannum (1982) are also shown. The moduli increase exponentially with increasing specimen density and are fit well by the Sjaardema and Krieg (1987) equation,

$$K = c \cdot \exp(b \cdot \rho)$$

where K is bulk modulus, D is density, and b and c are fitting constants. The values of b and c are 6.53 and 0.176, respectively, as given in Sjaardema and Krieg (1987), and 5.69 and 0.101, respectively, for the new fit to the data shown in Figure 5.

Microstructural Observations

Optical and scanning electron microscopy (SEM) were used to characterize the tamped salt and reconsolidated salt. "Tamped" refers to the salt mass after it has been compacted in the chamber, and "reconsolidated" refers to the tamped salt after it has been subjected to compressive stresses (usually hydrostatic) in the laboratory. A Zeiss photomicroscope was used for the optical work, and a JOEL JSM-840 A was used for the SEM observations. Substructures documented here are considered preliminary due to the limited scope of this study, but are nonetheless representative.

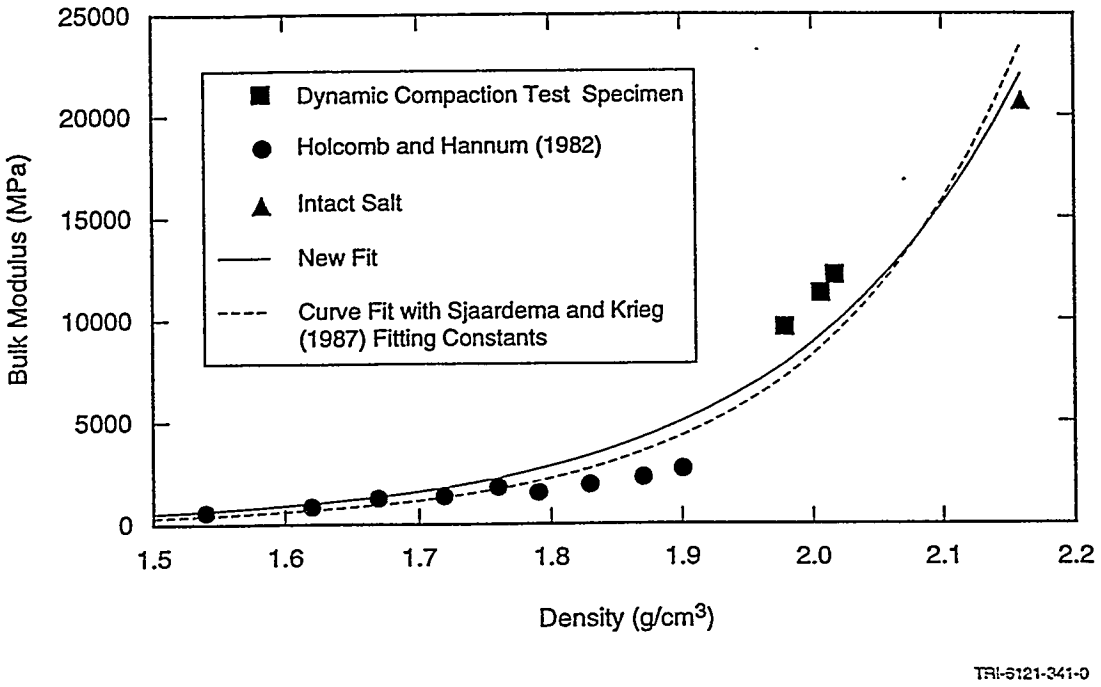

Figure 5. Bulk Modulus versus Density for Compacting Crushed Salt.

Optical microscopy used 6 polished petrographic thin sections. The contrast between tamped and reconsolidated salt is evident in two representative photomicrographs shown in Figures 6 and 7. Tamped salt shown in Figure 6 has a fractional density of 0.9. The loose, mine-run aggregate is densified by comminution during tamper impact followed by compression of fine (<10 microns) powder between larger grains. The largest grains remaining after compaction are of the order of 1 mm. Cataclasis is evidenced, at least from optical observations, by the sharp cubic cleavage and lack of distortion within the crystal lattice. Zones of minute grains exhibit birefringence, highlighting interstices between cubic faces. Figure 7 shows a thin section of reconsolidated salt (i.e., the tamped salt of Figure 6 after application of hydrostatic pressure) that has achieved a density of approximately 0.98. The fine powder has much less birefringence because of tight suturing of grain boundaries. Void space is eliminated by significant transport of material through pressure solution and reprecipitation.

Scanning electron micrographs (SEMs) further reveal densification processes. Thin sections did not produce suitable samples for SEM observations, so remnant plugs from sectioning were used. Therefore tamped and reconsolidated SEM specimens were identical to the thin section material. Plugs were broken by finger pressure, and the fractured surfaces were examined. Optical features are consistent with the electron images.

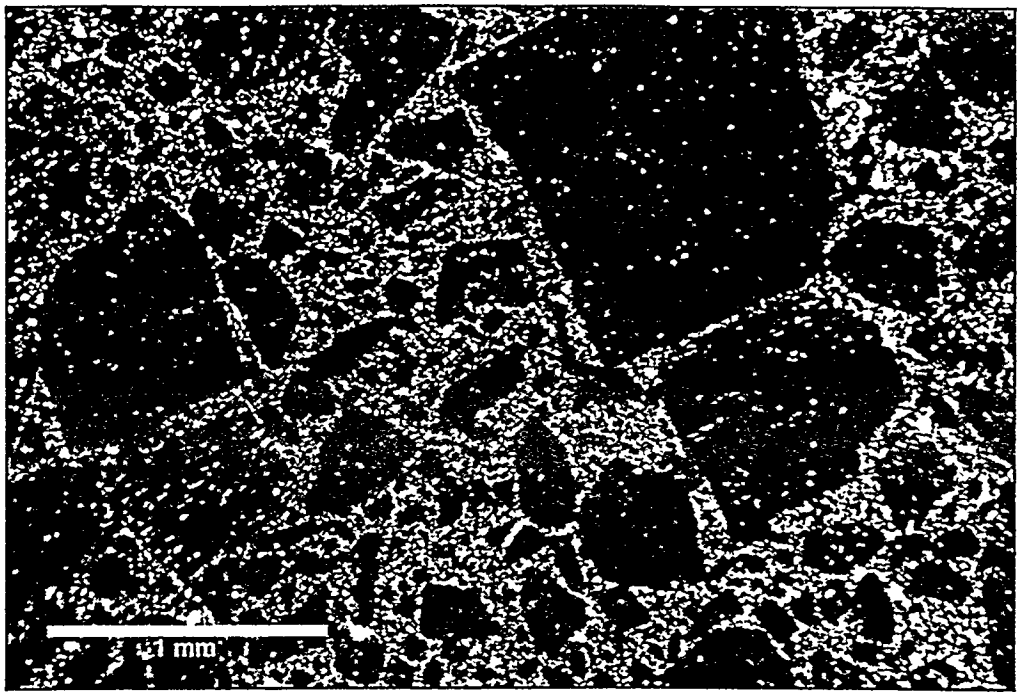

TRI-6121-342-0

Figure 6. Tamped Crushed Salt.

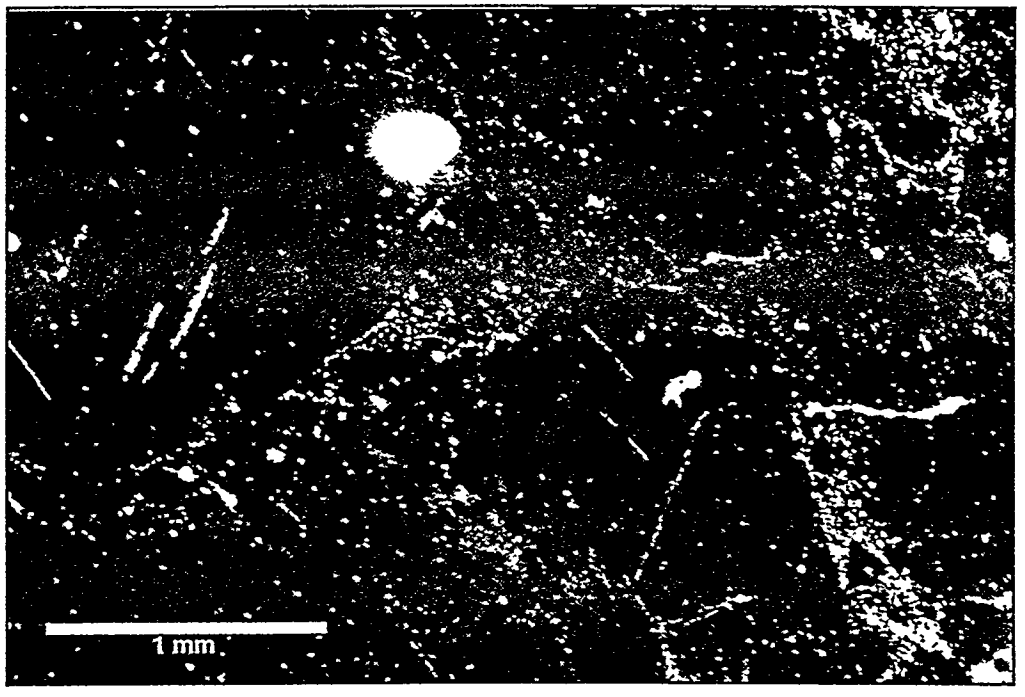

TRI-6121-343-0

Figure 7. Reconsolidated Crushed Salt.

Three SEM photomicrographs presented here capture essential features of tamped and reconsolidated crushed salt. Figure 8 shows the grain assemblage of compacted crushed salt immediately after if has been tamped (0.90 fractional density). The surface (top) of the sample shows grain boundaries separated cleanly without appreciable tensile cleavage. Grain boundaries are relatively closed, demonstrating that compaction was effective in producing a gradation of material that packed together well. No evidence of plasticity, pressure solution, or dislocation motion is observed. In contrast, Figure 9 shows the material from Figure 8 at the same magnification (1100×) after it has been reconsolidated to about 0.98 fractional density. Notice the sharpness of the top of the grains. As the plugs were broken, cohesion was sufficient to promote tensile cleavage. The process of pressure solution and redeposition is clearly evident on most grain contacts. On the basis of these photomicrographs, one can conclude that pressure solution/redeposition is actively transporting mass. Moreover, plastic mechanisms within each grain also contribute to reduction of void space. Sharp linear glide bands and wavy cross-slip bands are evident in many grains.

Figure 10 shows a highly deformed salt grain. This photomicrograph illustrates large strain accommodated by slip. It is interesting to note that the glide planes eventually gave rise to a fault within the grain. Pressure solution appears to dominate void reduction during reconsolidation, but glide is also an operative mechanism. These microstructural observations are consistent with observations of pressure solution or plasticity-induced solution transfer described in Brodsky et al. (1995) for reconsolidated crushed salt. Constitutive models evaluated by Callahan et al. (1996) are formulated for these processes.

SUMMARY AND CONCLUSIONS

Laboratory tests on compacted mine-run crushed salt from intermediate- and large-scale dynamic compaction tests show that fractional densities ranging between 0.85 and 0.90 can be easily achieved. *In situ* permeabilities of the dynamically compacted salt mass averaged 9×10^{-14} m^2, and laboratory test specimens manufactured from the dynamically compacted salt ranged from 10^{-12}• m^2 to 10^{-15}• m^2. Reconsolidation through application of uniform compressive stresses increased density and decreased permeability. A linear least square fit to the existing data is presented for permeability as a function of density as fractional density increases from 0.90 to 1.00. Bulk modulus increases exponentially with density and can be described by the Sjaardema and Krieg (1987) equation. Densification occurs by pressure solution at grain boundaries and dislocation glide within individual grains.

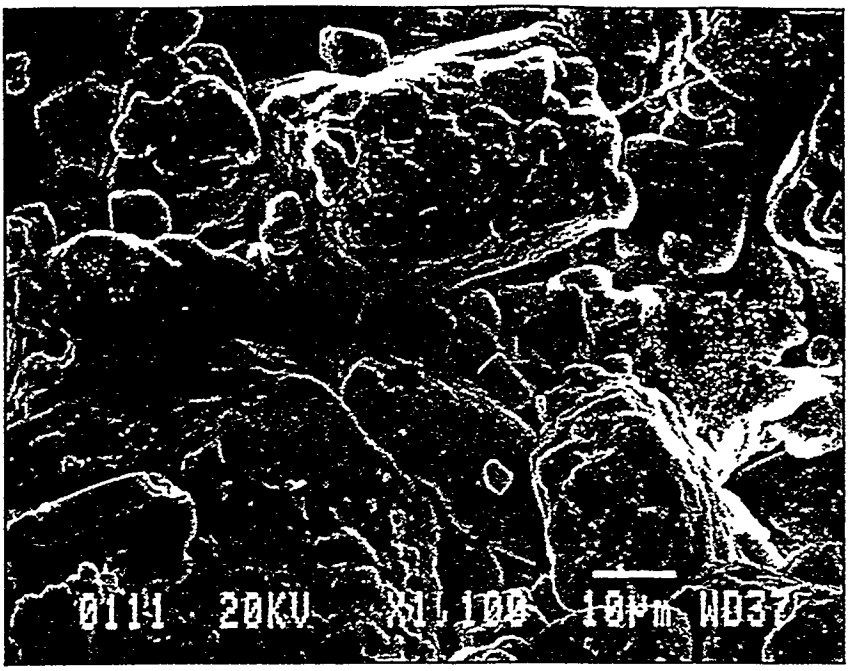

TRI-6121-344-0

Figure 8. Tamped, Unreconsolidated Crushed Salt.

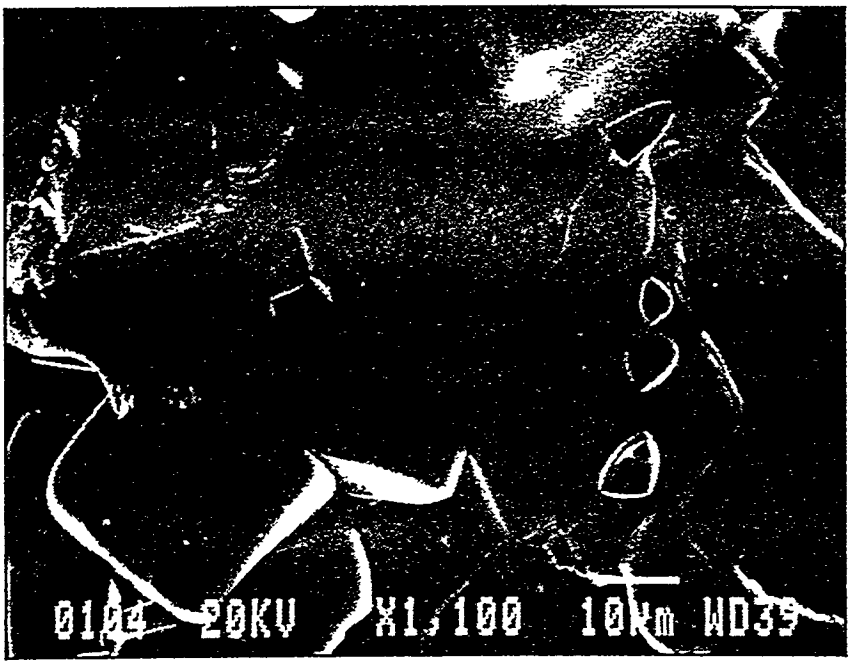

TRI-6121-345-0

Figure 9. Pressure Solution and Redeposition Features of Reconsolidated Salt.

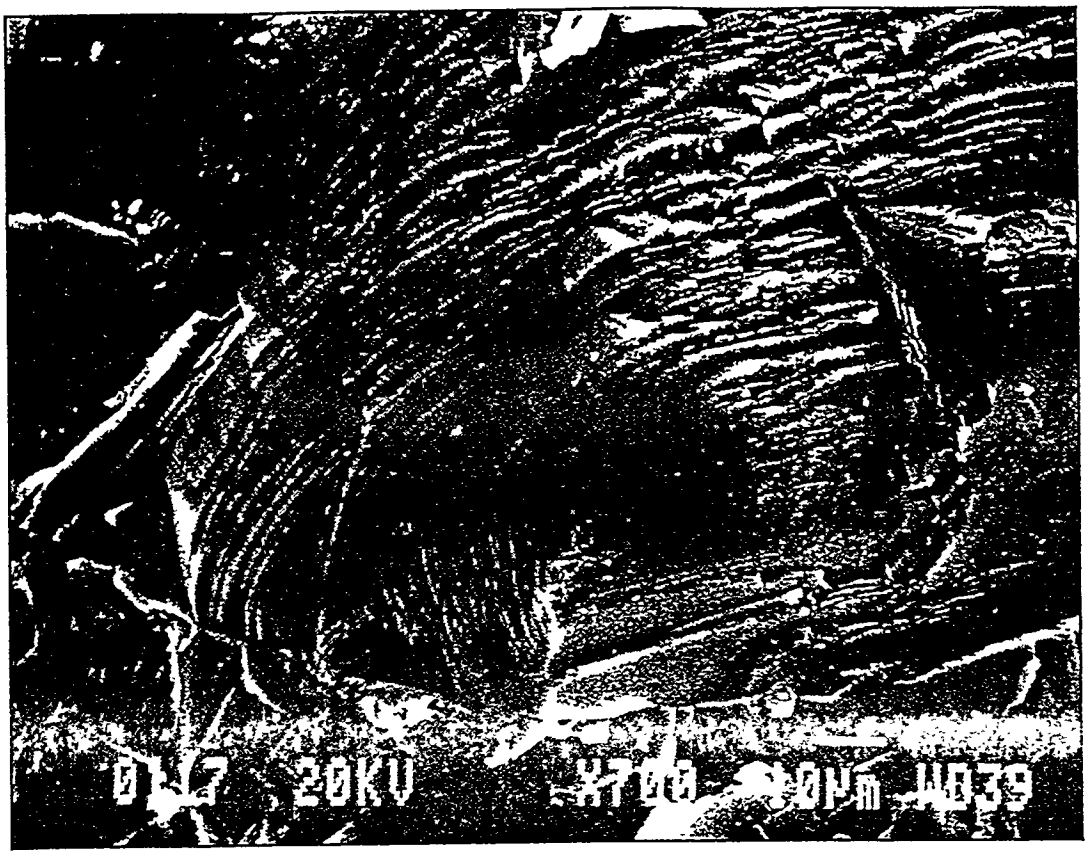

Figure 10. Slip Planes Exhibiting Large Strain.

REFERENCES

Brodsky, N.S. 1994. *Hydrostatic and Shear Consolidation Tests with Permeability Measurements on Waste Isolation Pilot Plant Crushed Salt.* SAND93-7058. Albuquerque, NM: Sandia National Laboratories.

Brodsky, N.S., D.H. Zeuch, and D.J. Holcomb. 1995. "Consolidation and Permeability of Crushed WIPP Salt in Hydrostatic and Triaxial Compression," *Proceedings of the 35th US Symposium on Rock Mechanics, Reno NV, June 5-7, 1995.* Eds. J.J.K. Daemen and R.A. Schultz. Brookfield, VT: A.A. Balkema. 497-502.

Callahan, G.D., M.C. Loken, L.D. Hurtado, and F.D. Hansen. 1996. "Evaluation of Constitutive Models for Crushed Salt," *Proceedings of the 4th Conference on the Mechanical Behavior of Salt, Montreal, QC, Canada, June 17-18, 1996.* SAND96-0796C. Albuquerque, NM: Sandia National Laboratories.

Hansen, F.D., and E.H. Ahrens. 1996. "Large-Scale Dynamic Compaction of Natural Salt," *Proceedings of the 4th Conference on the Mechanical Behavior of Salt,* June, 1996. *Montreal, QC, Canada, June 17-18, 1996.* SAND96-0796C. Albuquerque, NM: Sandia National Laboratories.

Hansen, F.D., E.H. Ahrens, V.C. Tidwell, J.R. Tillerson, and N.S. Brodsky. 1995. "Dynamic Compaction of Salt: Initial Demonstration and Performance Testing," *Proceedings of the 35th U. S. Symposium on Rock Mechanics, Reno, NV, June 5-7, 1995.* Eds. J.J.K. Daemen and R. A. Schultz. Brookfield, VT: A.A. Balkema. 755-760.

Holcomb, D.J., and D.W. Hannum. 1982. *Consolidation of Crushed Salt Backfill Under Conditions Appropriate to the WIPP Facility.* SAND82-0630. Albuquerque, NM: Sandia National Laboratories.

Holcomb, D.J., and M.E. Shields. 1987. *Hydrostatic Creep of Crushed Salt with Added Water.* SAND87-1990. Albuquerque, NM: Sandia National Laboratories.

Klinkenberg, L.J. 1941. "The Permeability of Porous Media to Liquids and Gases," *API Drilling and Production Practice.* 200-213.

Sjaardema, G.D., and R.D. Krieg. 1987. *A Constitutive Model for the Consolidation of WIPP Crushed Salt and Its Use in Analyses of Backfilled Shaft and Drift Configurations.* SAND87-1977. Albuquerque, NM: Sandia National Laboratories.

US Department of Energy. 1995. *Waste Isolation Pilot Plant Sealing System Design Report.* DOE/WIPP-95-3117. Carlsbad, NM: Waste Isolation Pilot Plant.

ACKNOWLEDGMENTS

The authors would like to thank Mr. Rodger Arnold (of RE/SPEC Inc.) for performing the density and permeability measurements, Mr. Steven B. Olsberg (also of RE/SPEC Inc.) for performing the difficult task of specimen preparation, and Mr. Kirby Mellegard (also of RE/SPEC Inc.) for developing the test-control software.

NOTES

[1] Work supported by US Dept. of Energy (DOE) under contract DE-AC04-94AL85000.

[2] A DOE facility.

DISCLAIMER